

**DESIGN OF DIELECTRIC RESONATOR ANTENNA FOR WIRELESS  
COMMUNICATION**

**By**

**MOHAMADARIFF BIN OTHMAN**

**Thesis submitted in fulfillment of the requirements  
for the degree of  
Master Of Science**

**UNIVERSITI SAINS MALAYSIA**

**May 2009**

## ACKNOWLEDGEMENTS

### **In the name of Allah, Most Gracious, Most Merciful.**

Praise be to Allah s.w.t for giving me the strength and guide me through thick and thin. First and foremost, my greatest honor and appreciation go to Dr Mohd Fadzil bin Ain, my supervisor for his tireless dedication, thoughts, encouragement and suggestions in guiding me to complete this thesis. Special thanks to Prof Syed Idris Syed Hassan who is a well-known legend in the field of antenna for his ideas and reviewing my thesis and also to all the member of WMRC group. It has been a great privilege to be a part of this group.

It is also my pleasure to thank Prof Zainal Arifin Ahmad and Dr Ansor, my co-supervisors for being such a great help not only for reviewing the thesis but more importantly for their constructive criticism and advices especially in the material aspect. I would like also to extend my thanks to Dr Srimala and Dr Sabar as well as Kia Ling, Azwadi and Nik Akmar for helping me to fabricate the dielectric material.

Special thanks to Prof Madya Dr. Othman Sidek (director of the CEDEC center) and his Research Officer, Mr. Mohd Shukri, in allowing me to use Network Analyzer. My gratitude also goes to the technicians, En. Abdul Latip and En. Elias for their endless assistant. I am also greatly indebted to the Mr Azwan for introducing me with Dr Fadzil Ain and path the way for this very interesting project.

Last but not least, I would like to thank my mother and father, who have always encouraged me to strive for my best in this project. Without their prayer and caring, this thesis can't be completed.

## TABLE OF CONTENTS

<b>TITLE</b> .....	i
<b>ACKNOWLEDGEMENT</b> .....	ii
<b>TABLE OF CONTENTS</b> .....	iii
<b>LIST OF TABLES</b> .....	vii
<b>LIST OF FIGURES</b> .....	viii
<b>LIST OF ABBREVIATION</b> .....	xiv
<b>ABSTRAK</b> .....	xv
<b>ABSTRACT</b> .....	xvii

### CHAPTER ONE : INTRODUCTION

1.1 Introduction.....	1
1.2 Problem Statement.....	3
1.3 Objective.....	5
1.4 Scope Of Project.....	6
1.5 Thesis Organization.....	8

### CHAPTER TWO : LITERATURE REVIEW

2.1 Challenges.....	9
2.2 Dielectric Resonator Antenna.....	12
2.2.1 Overview on Dielectric Resonator Antenna.....	12
2.2.2 Features.....	16
2.3 Method of Coupling.....	17
2.3.1 Microstrip line.....	17
2.3.2 Coaxial Probe.....	18
2.3.3 Slot Aperture.....	18
2.3.4 Coplanar waveguide.....	19
2.3.5 Dielectric Image Guide.....	19
2.4 Analyses of the DRA .....	20
2.4.1 Resonant Frequency.....	20
2.4.2 Resonant Modes.....	21

2.5 Low Profile and Small DRAs.....	27
2.6 Broadband DRAs.....	34
2.7 Dielectric Material .....	40
2.7.1 Introduction.....	40
2.7.2 Dielectric Properties.....	40
2.8 Dielectric Material Preparation for DRA.....	42
2.8.1 Powder Preparation.....	42
2.8.2 Mixing and Milling.....	43
2.8.3 Calcination.....	44
2.8.4 Pressing.....	45
2.8.5 Sintering.....	45
2.9 Characterization of Dielectric Material .....	46
2.9.1 X-ray Diffraction.....	46
2.9.2 Scanning Electron Microscopy.....	47
2.10 Simulation.....	48
2.10.1 Introduction.....	48
2.10.2 CST Studio Suite.....	48
2.10.3 CST Microwave Studio.....	50
2.11 Conclusion.....	53

### **CHAPTER THREE : METHODOLOGY**

3.1 Introduction.....	55
3.2 Design Specifications.....	57
3.2.1 Dielectric Material .....	57
3.2.2 Coupling Method .....	57
3.2.3 CCTO DRA.....	58
3.2.4 TiO DRA.....	59
3.3 Configuration of CST for DRA.....	61
3.3.1 Setting of Dielectric Substrate .....	61
3.3.2 Setting of Microstrip Feeder .....	63
3.3.3 Defining of Waveguide Port.....	65
3.3.4 Defining of Boundary Conditions.....	66
3.3.5 Far-field Monitor.....	67

3.3.6 Transient Solver.....	69
3.4 Dielectric Resonator Antenna Design.....	70
3.4.1 CCTO Dielectric Resonator Antenna .....	70
3.4.1.1 CCTO DRA with different diameter of pellets.....	71
3.4.1.2 CCTO DRA with silver paste.....	73
3.4.1.3 CCTO DRA with ring shape loading strip.....	75
3.4.2 Titanium Oxide Dielectric Resonator Antenna.....	76
3.4.2.1 Cylindrical TiO <sub>2</sub> DRA.....	76
3.4.2.2 Rectangular TiO <sub>2</sub> DRA.....	79
3.4.2.3 Circular sector TiO <sub>2</sub> DRA.....	80
3.4.3 Wideband Dielectric Resonator Antenna for Ku-Band Application.....	81
3.5 Fabrication of Microstrip Feeder.....	84
3.6 Dielectric Resonator Fabrication.....	84
3.6.1 Raw Material.....	86
3.6.2 Solid State Reaction.....	86
3.6.3 Composition Preparation.....	87
3.6.4 Mixing and Milling.....	87
3.6.5 Calcination.....	88
3.6.6 Pressing.....	89
3.6.6.1 CCTO powder.....	89
3.6.6.2 TiO <sub>2</sub> powder.....	90
3.6.7 Sintering.....	91
3.6.7.1 CCTO powder.....	91
3.6.7.2 TiO <sub>2</sub> powder.....	92
3.7 Dielectric Properties Characterization.....	92
3.7.1 Scanning Electronic Microscope.....	93
3.7.2 X-Ray Diffraction.....	93
3.7.3 Density and porosity determination.....	94
3.8 Dielectric Properties Measurement.....	95
3.8.1 Dielectric Properties at High Frequency.....	96
3.9 S-Parameter Measurement.....	98
3.10 Antenna Radiation Pattern Measurement.....	99

3.11 Conclusion.....	101
----------------------	-----

**CHAPTER FOUR : RESULTS AND DISCUSSION**

4.1 CCTO Dielectric Resonator Antenna.....	103
4.1.1 XRD analysis .....	103
4.1.2 SEM analysis .....	106
4.1.3 Density Determination .....	107
4.1.4 CCTO Dielectric Properties.....	108
4.1.5 Dielectric Properties at High Frequency.....	110
4.1.6 Simulated and Measured CCTO DRA.....	113
4.1.6.1 CCTO DRA with Pellet of 10.66 mm diameter.....	113
4.1.6.2 CCTO DRA with Pellet of 11.55 mm diameter.....	118
4.1.6.3 Comparison between Different Diameter of Pellet.....	123
4.1.6.4 CCTO DRA with Silver Paste.....	127
4.1.6.5 Comparison between Pellet With and Without Silver Paste ...	132
4.1.6.6 CCTO DRA with Ring-shape Strip Loading.....	135
4.1.7 Summary on the Design of CCTO Dielectric Antenna.....	143
4.2 TiO <sub>2</sub> Dielectric Resonator Antenna.....	145
4.2.1 XRD analysis.....	145
4.2.2 SEM analysis.....	146
4.2.3 Density Determination.....	148
4.2.4 TiO <sub>2</sub> Dielectric Properties.....	149
4.2.5 Dielectric Properties at High Frequency.....	151
4.2.6 Simulated and Measured TiO <sub>2</sub> DRA.....	153
4.2.6.1 Cylindrical TiO <sub>2</sub> DRA.....	153
4.2.6.2 Rectangular TiO <sub>2</sub> DRA.....	158
4.2.6.3 Circular TiO <sub>2</sub> DRA.....	163
4.2.6.4 Comparison between Different Shape of TiO <sub>2</sub> DRA.....	168
4.2.7 Summary on the Design of TiO <sub>2</sub> Dielectric Antenna.....	174
4.3 ZrSnTiO Dielectric Resonator Antenna.....	175
4.3.1 Wideband DRA for Ku-Band Application .....	176
4.3.2 Summary on the Design of ZrSnTiO Dielectric Resonator Antenna.....	181
4.4 Conclusion.....	182

<b>CHAPTER FIVE : CONCLUSSION AND FUTURE WORK</b>	
5.1 Conclusion.....	183
5.2 Future work.....	185
<b>REFERENCES.....</b>	<b>187</b>
<b>LIST OF PUBLICATION.....</b>	<b>193</b>
<b>ACHIEVEMENTS.....</b>	<b>194</b>
<b>APPENDICES.....</b>	<b>195</b>

## LIST OF TABLES

Table 2.1	Measured resonance frequency and bandwidth of low profile rectangular DRA
Table 2.2	Bandwidth Technique Used in DRA
Table 3.1	Characteristics of the dielectric substrate
Table 3.2	Parameter of the substrate and ground plane design
Table 3.3	Parameters of the microstrip line
Table 3.4	Parameter setting for the CCTO Dielectric Resonator Antenna
Table 3.5	Parameter setting for cylindrical TiO <sub>2</sub> Dielectric Resonator Antenna
Table 3.6	Parameter setting for the ZrSnTiO Dielectric Resonator Antenna
Table 4.1	Densities of CCTO samples
Table 4.2	Summary of the Design on CCTO DRA with 10.66 mm diameter
Table 4.3	Summary of the Design on CCTO DRA with 11.55 mm diameter
Table 4.4	Summary on the Design of CCTO DRA with silver paint
Table 4.5	Summary on the Design of CCTO DRA with strip loading
Table 4.6	Summary of the Design on Cylindrical TiO <sub>2</sub> DRA
Table 4.7	Summary of the Design on Rectangular TiO <sub>2</sub> DRA
Table 4.8	Summary of the Design on Circular Sector TiO <sub>2</sub> DRA
Table 4.9	Comparison result for Measured and Simulated ZrSnTiO DRA



## LIST OF FIGURES

- Figure 1.1 Implementation of the project
- Figure 2.1 Geometry of cylindrical dielectric antenna
- Figure 2.2 Cylindrical CCTO DRA
- Figure 2.3 Geometry of Rectangular DRA
- Figure 2.4 Geometries of Dielectric Resonator Antenna
- Figure 2.5 Microstrip line coupling to DRA
- Figure 2.6 Probe coupling to DRA
- Figure 2.7 Slot aperture coupling to DRA
- Figure 2.8 Electric field distribution for  $TE_{01}$  (a) E-field (b) H-field
- Figure 2.9 Electric field distribution for  $HEM_{11}$  (a) E-field (b) H-field
- Figure 2.10  $HEM_{11}$  mode (a) Electric field distribution (b) Magnetic field distribution
- Figure 2.11 Structure of probe feed cylindrical and rectangular DRA
- Figure 2.12 Field radiation models of microstrip line-coupled DRA
- Figure 2.13 Geometry of DRA fed by microstrip transmission line
- Figure 2.14 Electrically small antenna
- Figure 2.15 Top and side view of low-profile rectangular DRA
- Figure 2.16 Top view of circular sector DRA
- Figure 2.17 Top view of the Off Center Ring DRA
- Figure 2.18 Compact DRA with metallic plate
- Figure 2.19 Measured SWR of the antenna with different thickness of metal plate
- Figure 2.20 Cylindrical and half cylindrical DRA
- Figure 2.21 Stacked DRA
- Figure 2.22 Stub matching technique

- Figure 2.23 Strip-fed loading technique
- Figure 2.24 Two half DRAs
- Figure 2.25 Electric dipole structure
- Figure 2.26 Circuit configuration for the dielectric material
- Figure 2.27 Schematic illustration of SEM operation
- Figure 2.28 CST DESIGN ENVIRONMENT interface
- Figure 2.29 CST MICROWAVE STUDIO
- Figure 2.30 Parameter sweep tool box
- Figure 3.1 Flow Chart of the overall design process
- Figure 3.2 Setting for material parameter
- Figure 3.3 Dielectric Substrate (green) and Ground plane (yellow)
- Figure 3.4 Impedance Calculation dialog box
- Figure 3.5 Microstrip feeding of an antenna
- Figure 3.6 Waveguide Port
- Figure 3.7 Waveguide Port dialog box
- Figure 3.8 Boundary Conditions dialog box
- Figure 3.9 Far-field dialog box
- Figure 3.10 Transient Solver Parameters dialog box
- Figure 3.11 Structure of CCTO Dielectric Resonator Antenna. (a)Perspective view, (b) Top view
- Figure 3.12 Parameter Sweep setting box for CCTO DRA
- Figure 3.13 Structure of CCTO Dielectric Resonator Antenna with silver paint. (a)Perspective view, (b) Top view
- Figure 3.14 Structure of CCTO Dielectric Resonator Antenna with ring-shape silver paint (a) Perspective view, (b) Top view
- Figure 3.15 Structure of cylindrical  $\text{TiO}_2$  DRA (a) Perspective view, (b) Top view
- Figure 3.16 Parameter sweep box setting for cylindrical  $\text{TiO}_2$  DRA

- Figure 3.17 Structure of rectangular TiO<sub>2</sub> DRA (a) Perspective view, (b) Top view
- Figure 3.18 Structure of circular sector TiO<sub>2</sub> DRA (a) Perspective view, (b) Top view
- Figure 3.19 Structure of Wideband ZrSnTiO Dielectric Resonator Antenna. A) Perspective view, b) Top view
- Figure 3.20 Parameter Sweep setting box for ZrSnTiO Dielectric Resonator Antenna
- Figure 3.21 Flow Chart of the CCTO process
- Figure 3.22 Flow Chart of the TiO<sub>2</sub> process
- Figure 3.23 Grinding machine
- Figure 3.24 Calcination profile for CCTO powder.
- Figure 3.25 Uniaxial dry pressing machine.
- Figure 3.26 Sintering profile at temperature 1000 °C for 12 hours (Profile A)
- Figure 3.27 Sintering profile at temperature 1040 °C for 10 hours (Profile B)
- Figure 3.28 Sintering profile for BT and TiO<sub>2</sub> pellets
- Figure 3.29 Dielectric properties measurement using Impedance Analyzer and Dielectric Test Fixture
- Figure 3.30 Position of dielectric resonator to excite HEM<sub>11</sub>
- Figure 3.31 Equipment setup for S<sub>11</sub> measurement
- Figure 3.32 Equipment setup for radiation pattern measurement
- Figure 4.1 X-ray diffraction patterns for raw materials of (a) CaCO<sub>3</sub>, (b) CuO (c) TiO<sub>2</sub> powder
- Figure 4.2 XRD pattern of CCTO powder calcined at 900°C for 12 hours
- Figure 4.3 SEM images of fracture surface of CCTO sample sintered at 1000°C for 10 hours
- Figure 4.4 SEM images of fracture surface of CCTO sample sintered at 1040°C for 12 hours
- Figure 4.5 Dielectric constant of CCTO

- Figure 4.6 Tangent loss value of CCTO for different sintering temperature
- Figure 4.7 Measured resonant frequency for CCTO pellet at different sintering temperature (a) 1000 °C (b) 1040 °C.
- Figure 4.8 Geometry of the CCTO DRA with 10.66mm diameter for (a) simulated structure (b) fabricated structure
- Figure 4.9 Input impedance of CCTO DRA with 10.66mm diameter
- Figure 4.10 Return loss of CCTO DRA for 10.66 mm diameter
- Figure 4.11 Gain of CCTO DRA for 10.66 mm diameter
- Figure 4.12 Normalized radiation pattern at 3.7 GHz for 10.66mm pellet (a) E-plane (b) H-plane
- Figure 4.13 Geometry of the CCTO DRA with 11.55mm diameter for (a) simulated structure (b) fabricated structure
- Figure 4.14 Input impedance of CCTO DRA with 11.55mm diameter
- Figure 4.15 Return loss of CCTO DRA for 11.55mm diameter
- Figure 4.16 Normalized radiation pattern at 3.5 GHz for 11.55mm pellet (a) E-plane (b) H-plane
- Figure 4.17 Gain of CCTO DRA for 11.55 mm diameter
- Figure 4.18 Measured input impedance of CCTO DRA
- Figure 4.19 Measured return loss for different diameter of the CCTO pellets
- Figure 4.20 Radiation pattern of CCTO DRA for different diameter of pellet (a) E-plane (b) H-plane
- Figure 4.21 Geometry of the CCTO DRA with silver paste for (a) simulated structure (b) fabricated structure
- Figure 4.22 Input impedance of CCTO DRA with silver paste
- Figure 4.23 Return loss of CCTO DRA with metallic cap
- Figure 4.24 Gain of the CCTO DRA with silver paint
- Figure 4.25 Normalized radiation pattern at 2.3 GHz for 11.55mm pellet (a) E-plane (b) H-plane
- Figure 4.26 Measured return loss for CCTO DRA with and without silver paste

- Figure 4.27 Radiation pattern of CCTO with and without silver paste (a) H-plane (b) E-plane
- Figure 4.28 Geometry of the CCTO DRA with strip loading for (a) simulated structure (b) fabricated structure
- Figure 4.29 Input impedance of CCTO DRA with strip loading
- Figure 4.30 Return loss of CCTO DRA with strip loading
- Figure 4.31 Simulated radiation pattern for CCTO DRA with strip loading (a) E-plane, (b) H-plane
- Figure 4.32 Measured radiation pattern for CCTO DRA with strip loading (a) E-plane, (b) H-plane
- Figure 4.33 Gain of the CCTO DRA with strip loading
- Figure 4.34 XRD pattern of  $\text{TiO}_2$  at different sintering temperature (a)  $1000^\circ\text{C}$  (b)  $1100^\circ\text{C}$  (c)  $1200^\circ\text{C}$  and (d)  $1300^\circ\text{C}$
- Figure 4.35 SEM images of the  $\text{TiO}_2$  pellets sintered at a)  $1000^\circ\text{C}$ , b)  $1100^\circ\text{C}$ , c)  $1200^\circ\text{C}$  and d)  $1300^\circ\text{C}$  for 3 hours
- Figure 4.36 SEM images of fracture surface the  $\text{TiO}_2$  pellets sintered at a)  $1000^\circ\text{C}$ , b)  $1100^\circ\text{C}$ , c)  $1200^\circ\text{C}$  and d)  $1300^\circ\text{C}$  for 3 hours
- Figure 4.37 Densities of  $\text{TiO}_2$  pellets at different sintering temperature
- Figure 4.38 Dielectric constant of  $\text{TiO}_2$  at 1MHz
- Figure 4.39 Tangent loss value at 1MHz for different sintering temperature
- Figure 4.40 Measured resonant frequency for  $\text{TiO}_2$
- Figure 4.41 Geometry of the cylindrical  $\text{TiO}_2$  DRA (a) simulated structure (b) fabricated structure
- Figure 4.42 Input impedance of cylindrical  $\text{TiO}_2$  DRA
- Figure 4.43 Return loss for cylindrical shape  $\text{TiO}_2$  DRA
- Figure 4.44 Gain of the cylindrical  $\text{TiO}_2$  DRA
- Figure 4.45 Radiation patterns of cylindrical shape  $\text{TiO}_2$  for (a) E-plane (b) H-plane.
- Figure 4.46 Geometry of the rectangular  $\text{TiO}_2$  DRA (a) simulated structure (b) fabricated structure
- Figure 4.47 Input impedance of rectangular  $\text{TiO}_2$  DRA

- Figure 4.48 Return loss for rectangular shape TiO<sub>2</sub> DRA
- Figure 4.49 Gain of rectangular shape TiO<sub>2</sub> DRA
- Figure 4.50 Radiation patterns of rectangular shape TiO<sub>2</sub> for (a) E-plane (b) H-plane
- Figure 4.51 Geometry of the circular sector TiO<sub>2</sub> DRA for (a) simulated structure (b) fabricated structure
- Figure 4.52 Input impedance of circular shape TiO<sub>2</sub> DRA
- Figure 4.53 Return loss for circular sector TiO<sub>2</sub> DRA
- Figure 4.54 Gain of the circular sector TiO<sub>2</sub> DRA
- Figure 4.55 Radiation patterns of circular sector TiO<sub>2</sub> for (a) E-plane (b) H-plane
- Figure 4.56 Measured input impedance of different shape TiO<sub>2</sub> DRA
- Figure 4.57 Comparison of measured return loss between cylindrical, rectangular and circular shape TiO<sub>2</sub> DRA
- Figure 4.58 Gain of TiO<sub>2</sub> DRA.
- Figure 4.59 Simulated radiation pattern for different TiO<sub>2</sub> shape (a) E-plane, (b) H-plane
- Figure 4.60 Measured radiation pattern for different TiO<sub>2</sub> shape (a) E-plane, (b) H-plane
- Figure 4.61 Geometry of the wideband DRA (a) simulated structure (b) fabricated structure
- Figure 4.62 Input Impedance of the wideband DRA
- Figure 4.63 Return loss for wideband DRA
- Figure 4.64 Gain of wideband DRA
- Figure 4.65 Normalized radiation pattern at 11.9 GHz for wideband DRA (a) E-plane (b) H-plane

## LIST OF ABBREVIATIONS

3G	Third generation
ADS	Advanced Design System
CCTO	Calcium copper titanate
CST	Computer simulation technology
DR	Dielectric resonator
DRA	Dielectric resonator antenna
EDGE	Enhanced data rates for GSM evolution
GPRS	General packet radio service
GPS	Global positioning system
GSM	Global system for mobile communication
HE	Hybrid electric
HEM	Hybrid electromagnetic
HPBW	Half power bandwidth
HSDPA	High-speed downlink packet access
IP	Internet protocol
MCMC	Malaysian Communication and Multimedia Commission
MIC	Microwave Integrated Circuit
MIMO	Multiple input multiple output
MWS	Microwave Studio
RF	Radio Frequency
TE	Transverse electric
TiO <sub>2</sub>	Titanate
TM	Transverse magnetic
WLAN	Wireless local area network
ZrSnTiO	Zirconium tin titanate

## ABSTRAK

Disertasi ini membincangkan penghasilan antenna penyalun dielektrik (DRA) yang kecil dan padat di samping kajian terhadap bentuk penyalun dielektrik (DR) bagi DRA dan peningkatan terhadap jalur lebar DRA. Untuk mengurangkan saiz isipadu DRA, perekat perak digunakan. Ini boleh dilakukan dengan mengenakan perekat perak di atas permukaan DRA dan perbandingan dibuat diantara DRA yang ada dan tiada perekat perak. Untuk rekaan bagi DRA jalur lebar tinggi, dua pendekatan digunakan. Satu dengan menggunakan perekat perak dalam bentuk cincin dan satu lagi dengan menggunakan dua DR dengan serentak. Perekat perak bentuk cincin dikenakan di atas permukaan DR bagi menghasilkan kapasitans dan induktans tambahan bagi tujuan jalur lebar tinggi sebaliknya dua DR dengan pemalar dielektrik yang sama iaitu 37.1 digunakan untuk menghasilkan dua frekuensi jalunan yang akan bergabung untuk membentuk DRA jalur lebar yang tinggi. Kajian ke atas bentuk DRA melibatkan DR dalam bentuk bulat, empat segi dan sektor bulatan. Seterusnya, perbandingan di antara bentuk DR yang berlainan dibuat. Perisian yang dikenali CST Microwave Studio digunakan bagi mengenal pasti sifat DRA bagi setiap model. Setiap DR dihasilkan melalui kaedah tindak balas keadaan pepejal kecuali hanya DR ZrSnTiO yang telah siap sedia dalam bentuk bulat yang dibeli terus. Setiap DRA yang dihasilkan akan diuji dari segi galangan input, parameter S dan corak pancaran. DRA yang kecil beroperasi pada 2.46 GHz berjaya dihasilkan dengan menggunakan perekat perak. Frekuensi salunan berkurang dari 3.575 GHz kepada 2.46 GHz apabila DR diliputi dengan perekat perak. Dengan itu, DRA dengan perekat perak adalah lebih kecil dari DRA yang tiada perekat perak yang berfungsi pada frekuensi 2.46 GHz dengan corak pancaran yang tidak banyak beza. Untuk antenna berjalur lebar tinggi, perekat perak



berbentuk cincin di atas permukaan DR menghasilkan jalur lebar yang tinggi hingga 20% atau dalam 1 GHz. Namun, corak sinaran sedikit berbeza disebabkan oleh ragam yang dihasilkan mempunyai corak sinaran berbeza. DRA jalur lebar tinggi juga berjaya dihasilkan dengan menggunakan dua DR menghasilkan dua frekuensi salunan pada 11.92 GHz and 12.64 GHz dan seterusnya membentuk jalur lebar yang tinggi iaitu 8.87% atau 1.09 GHz. Akhir sekali, kajian yang dijalankan pada bentuk DRA menunjukkan bahawa tiga bentuk DR yang berlainan menghasilkan tiga frekuensi salunan. Ini menunjukkan bahawa bentuk DR di dalam struktur silinder, empat segi dan sektor bulatan mempunyai pengaruh besar terhadap persembahan DRA.

## ABSTRACT

This dissertation discussed on the design of small, compact dielectric resonator antenna (DRA) and the study on the shape of dielectric resonator (DR) for DRA as well as to enhance the bandwidth of DRA. In order to reduce the volume of DRA, silver paste is applied. This can be done by painting it on the surface of DRA and the comparison is made between the DRA with and without silver paste. For wideband DRA design, two approaches are implemented. One is by using silver paste in the form of ring shape and another one is by using two DRs simultaneously. Ring-shape silver paste is painted on the DR surface to produce additional capacitance and inductance for wideband operational DRA whereas two DRs with same permittivity of 37.1 are used to generate dual resonant frequencies which merge together to form wideband DRA. Investigation on the shape of DRA involved DR in the form of cylindrical, rectangular and circular sector. Subsequently, comparison between all different shapes of DR are made. For the purpose of obtaining invaluable insight on the design, CST Microwave Studio is used. Most of DR is made by using solid-state reaction while only ZrSnTiO DR which is already available in the form of cylindrical is straightly purchased. Each DRA design undergoes input impedance, S-parameter and radiation pattern measurement. Compact DRA operating at 2.46 GHz is achieved by utilizing silver paste. Resonant frequency is reduced from 3.575 GHz to 2.46 GHz once the DR is covered with silver paste. Hence, DRA with silver paste is smaller than DRA without silver paste when DRA operates at 2.46 GHz with no major different on the field pattern. For the wideband DRA, loading a strip in the form of ring on the surface of cylindrical DRA produces bandwidth of up to 20% or around 1 GHz. However, the radiation pattern is slightly different within the range of frequencies due to the modes

which produce different radiation pattern. Wideband DRA is also successfully designed by using two DRs resulted in two resonant frequencies of 11.92 GHz and 12.64 GHz and produced impedance bandwidth of 8.87 % or 1.09 GHz. Lastly, the study conducted on the shape of DRA revealed that three different shape of DR produces different resonant frequencies. This highlights that the shape of DR in the form of cylindrical, rectangular and circular sector DRA has big influences on DRA performance.

## **CHAPTER ONE**

### **INTRODUCTION**

#### **1.1 Introduction**

Over the past decades, wireless communication has experienced vast improvement and growth and will certainly continue to develop and expand its influence to the life of mankind. This development is due to the growth in information services and microelectronic devices which merge together to form highly integrated system and interactive multimedia applications. For instance, emailing, downloading from the internet and exchanging data over Bluetooth can be done within one device such as modern smart phones and handheld Personal Digital Assistant (PDAs) (Conti, 2007).

Furthermore, it is also almost for sure that the next generation wireless system will consist of a system with a set of different standard and technologies. This is the so-called ‘wireless dream’ of getting access in anyplace with any device and with any wireless standard. However, the whole wireless system comprise of many sub-systems which make it totally a complex system. In order to have smooth data exchanged by using any wireless device all of the sub-system in the transmitting and receiving part has to be perfect. For wireless communication systems, the antenna is one of the most crucial parts. It is caused by the fact than an antenna is the only structure for interfacing between guiding device and free-space surrounding it (Constantine, 1997). Hence, antennas are perhaps the most flexible, efficient, and vulnerable elements of wireless network or device (John, 2003). A good design of the antenna can improve overall

system performance and accommodate system requirement (Constantine, 1997). Together with upcoming fourth-generation (4G) cellular phones and wireless product and services, antenna can be found everywhere with different sizes and types for the specific application. The simplest one is wire antenna which can be connected to a transmitter or receiver system to form dipole, loop and helical antenna.

However, when it come to the millimeter wave application which covered high frequency range only few can live up to expectation. At these frequency, metallic antenna such as patch antenna and vivaldi antenna suffer more on conductor losses which can severely effected the performance of the antenna (Drossos et al., 1997). Other aspect such as portability and safety reason along with multi-functional antenna also come into account (Conti, 2006).

Consequently, new antenna technology which exploits the use of ceramic material as its resonator is presented in this thesis. This antenna is famously known as dielectric resonator antenna (DRA) and becomes an alternative antenna for the conventional one. It is resonant radiators fabricated from low-loss dielectric materials which can be formed to any shape such as cylindrical, rectangular and ring (Petosa et al., 1998). This antenna offers high degree of flexibility as many parameter such dielectric constant, shape and size can be adjusted to obtain optimum performances for a given application (Petosa, 2007).

## 1.2 Problem Statement

As time goes on, the whole wireless system become small and compact as well as the size of the antenna. A clear example of this scenario can be look at the antenna on the mobile in the early age. They utilize monopole antenna protruded outside the mobile case which can be easily broken as there is no shield to protect it if any accident occur. Nowadays, modern mobile antenna is embedded inside the mobile case to enhance the quality of the mobile in term of mobility, portability and low-profile (Upton and Steel, 2006).

In fact, low-profile and small antenna is really recommended for any communication system not only in mobile but also in military, medical or any system which is really based on wireless device to operate. For instance, in radar technology, small antenna is essential to reduce the weight of the radar, therefore, enable smooth mobility of the rotators driven by compact and small antenna (Kishk, 2003). Besides, conventional Yagi Uda antenna which can easily be found over the roof of each house is characterized by its big size, easily susceptible to damage and has many branches on either side. Hence, it is reasonable and practical if this antenna can be replaced with efficient, small and low-profile antenna while still maintaining its performance. In order to fix this problem, only two novel and low-profile antennas are highly suitable for the development of modern wireless communications. There are microstrip antenna and DRA. In the former, it suffers from conductor loss more than the DRA and this can degrade quality of the antenna (Drossos et al., 1997). One of the ways to reduce the size of the DRA is by using high permittivity dielectric material. However, using high permittivity material as dielectric resonator causes certain drawback to the performance of the DRA. As dielectric constant increase, the bandwidth tends to decrease (Kishk,

2003). Furthermore, flexibility is another point to take into account in any modern antenna design for wireless communication. Horn and vivaldi antenna are the type of directional antenna which normally have very high gain. This antenna, famously known to be used as a feed for reflectors and lenses and also as universal standard for gain measurements, cannot be adjusted to become omni directional antenna (Constantine, 1997). Similarly, helical antenna cannot become directional antenna without going to increase the length of the wire, therefore, cannot maintain a low-profile (Cuhaci et al., 1996). Almost all antennas do not possess high degree of flexibility which creates a lot of barrier to accommodate with any design requirement except DRA.

DRA offer a lot of appealing features which make it as an ideal candidate for every wireless application requiring high gain, circular polarization, omni directional pattern, low profile design and many more (Kishk, 2003; Petosa et al., 1998). Different feeding mechanism such as microstrip line and probes and various selection of dielectric material highlight its high degree of flexibility and versatility to facilitate with any design restriction and requirements (Petosa, 2007).

As stated before, many different wireless standards are available and another standard will emerge in the next future for communication device. Demand for the wireless device which can support multiple wireless standards keep on increasing. As a result, it requires that the same wireless device can support different frequency bands, therefore, increasing the device's functionality. Using multiple antennas to cover multiple bands cost a lot of money as well as space and time. Hence, the way out for this problem is to have a device with an antenna which can cover multi-band operation such as WLAN at 2.5 GHz, GPRS at 1.5575 GHz and many more. In short, wireless device with a wideband antenna.

### **1.3 Objective**

The objectives of this research are listed down as below:

1. To design low-profile and compact dielectric resonator antenna (DRA) and to study the effect of metal plate on the DRA in term of size, resonant frequency and radiation pattern. High permittivity material of higher than 20 are used to produce small DRA since its size is inversely proportional to the permittivity of material. The operational frequency of DRA is based on the size of mould being used. Study on metal plate involves placing the silver paint which acts as the metal plate on the surface of the DRA. Comparison is made between with and without silver paste to acquire frequency shifting.
2. To design wideband DRA by using multiple dielectric resonators at 10 GHz for satellite application. This design involves co-planar configuration with the same dimension of dielectric resonator are used. Two dielectric resonators are used as the basic for the DRA array design and to achieve high gain. Additionally, new form of parasitic patch on the dielectric resonator is used to gain wideband DRA at 5 GHz for WLAN application.
3. To study the effect of different shape of dielectric resonator such as rectangular, cylindrical and circular sector on the resonant frequency and radiation pattern of the DRA. As a result, this gives flexibility to control the frequency of DRA and make it possible to integrate with any existing technology by using different shape of dielectric resonator.



## 1.4 Scope of Project

The scope of this project focused on the design of the microstrip-fed DRA. All the design is excited with microstrip line because this feeding mechanism is the simplest and easiest among other feeder. This microstrip line is photo etched on the substrate from Roger Corporation, the Ultralam 2000 series with dielectric constant between 2.2 to 2.4.

The dielectric resonators used in this design are fabricated from three different materials. These dielectric materials are known as zirconium tin titanate (ZrSnTiO), calcium copper titanate (CCTO) and titanate ( $\text{TiO}_2$ ). ZrSnTiO dielectric resonator is bought from Tekelec Temex, E2000 series, with dielectric constant ranging from 37.1 to 37.6. The other two type's dielectric resonators are fabricated in the lab.  $\text{TiO}_2$  dielectric resonator is prepared from commercially available titanate while CCTO dielectric material from CCTO powder which undergone mixing, milling and calcinations process to produce pure CCTO powder. Later,  $\text{TiO}_2$  and CCTO dielectric resonator are measured to determine its dielectric constant and tangent loss value. After that, these resonators are used in the antenna and measurement process is conducted. The result is then analyzed and discussed. In order to facilitate fabrication work, simulation had been conducted before by using CST Microwave Studio. At the end, comparisons are made between the simulation and measurement results.

Basically, there are four major procedures in order to accomplish this project. A clear illustration is shown in the flow chart below.

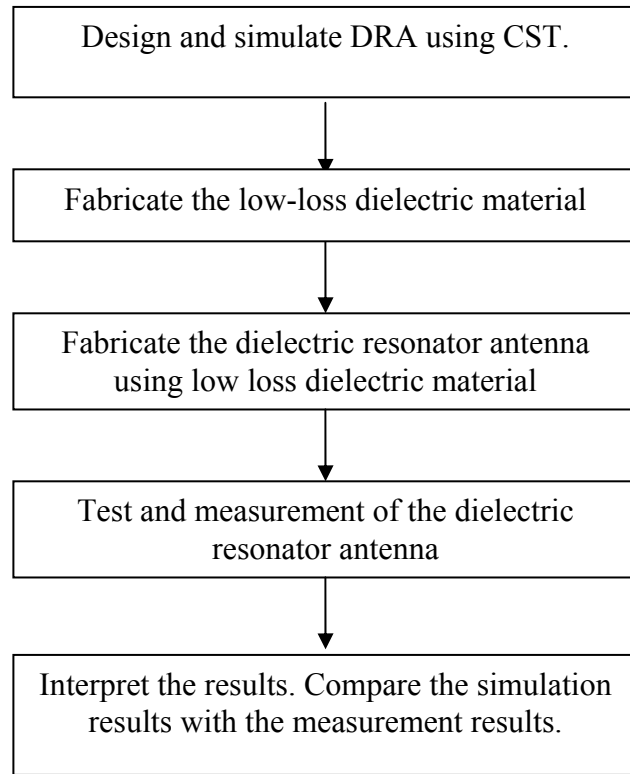


**Figure 1.1: Implementation of the project**

## **1.5 Thesis Organization**

The report has been divided into a total of five chapters. Chapter 1 begins with brief introduction of the recent trend in antenna technology and dielectric antenna in the wireless communication. This chapter also has laid out the background as to why this research was carried out and outlined the expected goals of the study.

Chapter 2 provides the critical study and thorough analysis into the principle of dielectric resonator antenna taken from previous research. This chapter focuses more on the small and low-profile DRA as well as broadband DRA as these are the main goal for this research.

Chapter 3 contained details description of experiment carried out. This includes the simulation procedure which was done using CST software and fabrication process to produce ceramic puck from different material composition. This ceramic puck is used as the dielectric resonator in antenna configuration.

Chapter 4 discusses in details result from both the measurement and simulation. The simulation results in term of S-parameter and radiation pattern have been generated. Various measurements for dielectric resonator antenna fabricated from different materials are also displayed and discussed. Comparison is made between measurement and simulation result.

Chapter 5 summarizes the result of the design on the size and bandwidth of DRA to analyze whether the aim of the project is achieved or not. At the end, some suggestions which can be carried out as the continuity on this project are presented

## **CHAPTER TWO**

### **LITERATURE REVIEW**

#### **2.1 Challenges**

It is stated that one of the 10 greatest communication inventions that changed the world forever is converged device. For examples, mobile phones that can have Internet access, TV programmers and GPS service and PCs that not only browse to the internet but also can make and receive IP phone calls (Conti, 2007). New and emerging converged devices in communication applications normally associated themselves with increasing data rates and wide frequency band required for service such as video-conferencing, direct digital broadcast, indoor wireless as well as new wireless standard demand (Petosa et al., 1998). Individual antenna assign for each portion of band for respective services occupy a lot of space, time and cost. Hence, it often preferable to use single antenna which can provides full coverage over the entire frequency range.

Moreover, it is expected that more new frequency bands to be added into modern communication network. If the current antenna system is not designed for the sufficient bandwidth to cover this new frequency band, it needs to be upgraded to cover these new bands. To make matter worse, probably it need to be replaced with new antenna. However, if a single antenna already has wide bandwidth which can spare several portion of band for the upcoming frequency bands, there is no need to replace it (Walker, 2007).

In recent years, the demand for wireless mobile communications has led not only to the development of antennas that are wider in bandwidth but also low profile as well as small in size (Saed and Yadla, 2006). To put it into nutshell, both of the size and bandwidth of the antenna should go side by side that of low profile and having wide bandwidth. This is more obvious when antenna need to be integrated with monolithic integrated circuit or MIC (Kumar et al., 2006). Because of the reduced size of the wireless device, antennas are physically and in most cases also electrically small (Wansch, 2002). A clear example of this scenario can be seen on the mobile phones which are being designed to be thinner, slimmer and narrower than ever before. Previously, the space available for the total RF section was approximately to  $600\text{mm}^2$  but is reduced to only half of  $300\text{mm}^2$  for 3G phone with multiple GSM, EDGE and HSDPA radios (Upton and Steel, 2006). As a result, antenna should be as small as possible but at the same time produce maximum antenna performance. The reasons behind designing small antenna are due to the more and more demand to improve the antenna design in term of size, low manufacturing cost and light in weight for better handling (Hui and Luk, 2005).

Antenna is also one of the crucial part in MIMO system since by using multiple antennas it can realize high capacity and transmission data rate (Xiao-Cong et al., 2005). In this system, multiple antennas at the transceivers of the communication system are employed. But when it comes to integrate MIMO systems into handhelds, several requirements for the antenna need to be considered. Waldschmidt et al., (2004) and (Min et al., 2007) show that it is possible to integrate several antennas into small hand-held devices using multi-channel MIMO antenna array. In order to create a MIMO antenna system on a wireless handy device, only small space is allocated, therefore, small and

compact antenna is really preferable. Besides, the efficiency of the antenna should be high to ensure long battery life as most of the terminals are battery-driven (Waldschmidt et al., 2005).

Furthermore, in radar system antenna is used to identify the moving objects accurately. In military operation, radar provides a critical advantage for the warfighter whether in most intense weather condition, terrain, dense jungle, or river system. For the next generation air defense systems, radar system need to be improved to support new Air Defense System which include high mobility and transportability, remote operation and increased sensitivity to detect smaller targets at longer ranges (Jr. et al., 2006). Besides, for the next 8 years, radar system will see tremendous changes due to the innovative system design which lead to a reduction in size and weight of radars (Jr. et al., 2006). Therefore, small and compact antenna is essential in radar to fulfill those requirements. Kishk (2003) stated the advantage of using small size array antenna element which contribute to the reduction on antenna weight and lead to the lighter rotators for the mechanical scanning and easy mobility. Apart from that, better resolution for image process also contributes to the high quality of radar. Both of these can be realized by utilizing wide frequency band of antenna (Kishk, 2003).

## **2.2 Dielectric Resonator Antenna**

### **2.2.1 Overview on Dielectric Resonator Antenna**

It has been almost 25 years since dielectric resonator antenna has come into existence in the wireless communication world (Long and O'Connor, 2007). However, before the emergence of this new radiator, dielectric resonator is famously known to be used in the microwave circuits such as filter and oscillator (Cohn, 1968; Petosa, 2007). It is due to its attractive features, for instance, small, stable and lightweight while at the same time can perform the same function as waveguide filters and resonant cavities which are expensive and difficult to adjust and maintain (Fiedziuszko, 2001). Because of this, DR is normally treated as an energy storage device rather than as a radiator.

It started in 1939 when R.D. Richtmyer, the person responsible on introducing the term “dielectric resonator”, found that unmetalized dielectric object can act as a microwave resonator. It becomes resonator due to the internal reflection of electromagnetic wave at the high dielectric constant material/air boundary to form a resonant structure. This results in confinement of energy within and in the vicinity of the dielectric material and form a standing wave with a specific field distribution at a unique frequency which is known as a mode. Details on the operating mode of DRA are given in the Section 2.4.2. In dielectric resonator, some part of the wave will leak through high dielectric constant material to low dielectric constant material (air) (Fiedziuszko, 2001).

For the filter application, the resonator is normally in the form of dielectric disk and is usually shielded. As in turn there will be no radiation and thus maintain a high quality factor which is required for the filter and oscillator application (Fiedziuszko, 2001). However, at the same time microwave circuit community face problem in dealing with the radiation leak out from the cylindrical DR in microwave circuit. Besides, it is

discovered that at higher frequencies, microstrip antenna became less efficient due to the higher ohmic losses (Long and O'Connor, 2007).

As a result, in the early 1980s, Stuart Long and Liang Shen pioneered the effort on this new radiating element from the dielectric resonator that is later known as dielectric resonator antenna (Long et al., 1983). According to (Mongia et al., 1993) when dielectric resonator is placed in an open environment it can produce low values of radiation Q-factor and can be used as a resonant antenna. Figure 2.1 shows the first ever dielectric resonator antenna design.

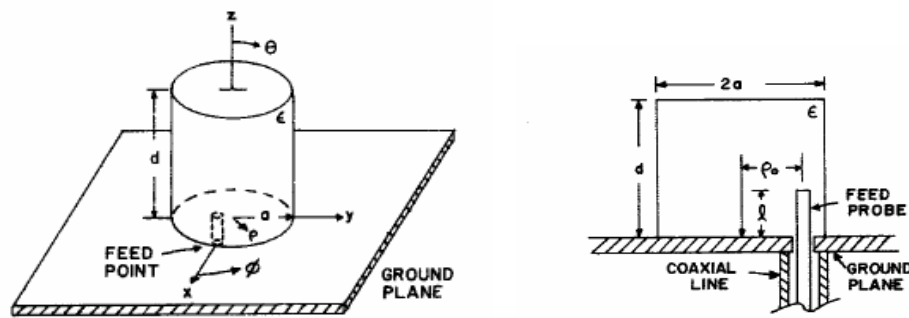


**Figure 2.1: Geometry of cylindrical dielectric antenna (Long et al., 1983)**

Since, open DR is found can radiate so it can be used also as an antenna which is known as dielectric resonator antenna (DRA). Dielectric resonator antenna is a resonant radiator fabricated from low loss dielectric material and can be formed into various shapes such as cylindrical and rectangular. Its resonant frequency is proportional to the size, shape and dielectric constant of the dielectric material (Cuhaci et al., 1996; Petosa et al., 1998). Since, DRA is fabricated from ceramic material, therefore, many dielectric material can be used for the dielectric resonator fabrication where the first temperature



stable and low-loss ceramic manage to be developed is Barium Tetratitanate (Fiedziuszko, 2001).

Ameida et al., (2007) had investigated CCTO ceramic material as a new cylindrical DRA operating around 4.6 GHz. In this study CCTO ceramic phase is synthesized by microwave heating and yield dielectric constant of 62 and bandwidth of 9.4%. Figure 2.2 shows that CCTO material is sintered in cylindrical-shape and excited by a coaxial probe.

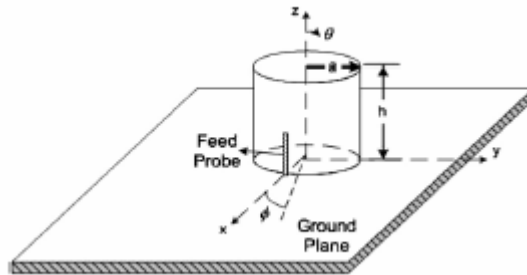


**Figure 2.2: Cylindrical CCTO DRA (Almeida et al., 2007)**

Another material known as  $\text{Ca}_5\text{Nb}_2\text{TiO}_{12}$  is also used to fabricate the Dielectric Resonator (Mridula et al., 2004). This ceramic material has dielectric constant of 48, fabricated in the form of rectangular by the conventional solid-state ceramic route and sintered in the temperature range of  $1500^\circ\text{C}$  to  $1600^\circ\text{C}$ . This DRA was design for the wideband application by loading a stub of length of 2.7 cm at the top of the microstrip line as shown in the Figure 2.3.

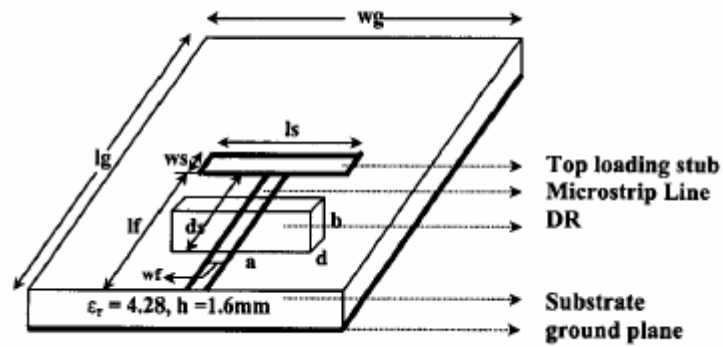


**Figure 2.3: Geometry of Rectangular DRA (Mridula et al., 2004)**

It is proven by Mridula et al., (2004) that by changing the shape of DR, resonant frequency can be varied. Hence, ceramic material is also fabricated in a variety of shape to accommodate with different application and at the same time maintaining the performance of antenna (Kishk, 2003). Some of the shape is shown in the Figure 2.4. The details on the shape of DR to produce low-profile and small DRA will be discussed later in Section 2.5.

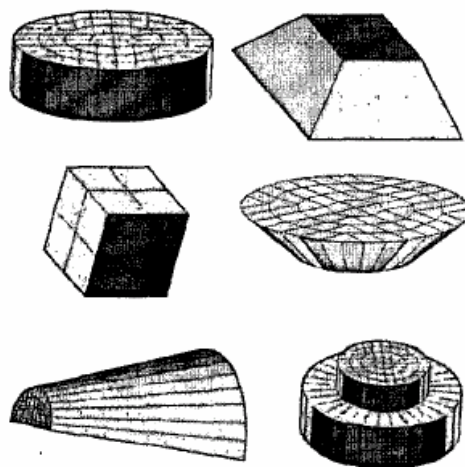


**Figure 2.4: Geometries of Dielectric Resonator Antenna (Kishk, 2003)**

### 2.2.2 Features

Dielectric resonator antenna has many appealing features which make it as one of the alternative antenna technology in wireless communication field (Petosa et al., 1998). Some of the attractive features are listed below (Cuhaci et al., 1996; Kishk, 2003; Petosa, 2007; Petosa et al., 1998).

a) The size of the DRA is proportional to the dielectric constant of the material which can be varied from about 8 to 100 allowing more control over the size and bandwidth of DRA. DRA size decreases when dielectric constant increases.

b) DRA suffers from almost no dissipation losses and nonexistence of surface wave losses which contribute to high radiation efficiency and wide bandwidth.

c) Various excitation mechanisms can be used (probes, slots, microstrip lines) to excite DRA which make it easy to integrate with many existing technology.

d) Various shape of dielectric resonator can be designed (triangular, hemispherical, etc.) offering more degrees of freedom to the design.

e) Various modes can be excited leading to the different radiation characteristic. These modes can be controlled by using different excitation mechanism.

## 2.3 Method of Coupling

One of the advantages of using DRA is the capability to be excited with different feeding mechanism such as microstrip line, probe and coplanar waveguide (Kishk, 2003). The selection of the feed and its position play important role to determine the mode which later contributes in determining the input impedance, return loss as well as radiation characteristic of the antenna (Petosa, 2007).

### 2.3.1 Microstrip line

A common method for coupling to dielectric resonator antenna in microwave circuit is by microstrip line (Petosa, 2007). The amount of coupling from the microstrip line can be controlled by adjusting the lateral distance of the DRA with respect to the microstrip line and on the dielectric constant of the dielectric substrate (Rezaei et al., 2006b). Otherwise, the maximum amount of coupling is significantly reduced. There are two methods of microstrip line coupling; side coupling or direct coupling (Petosa, 2007). Figure 2.5 shows microstrip line coupling to the DRA. This feeding mechanism offers ease integrations with the other microwave circuit but produce unwanted air gap between the DRA and the substrate (Luk et al., 1999).

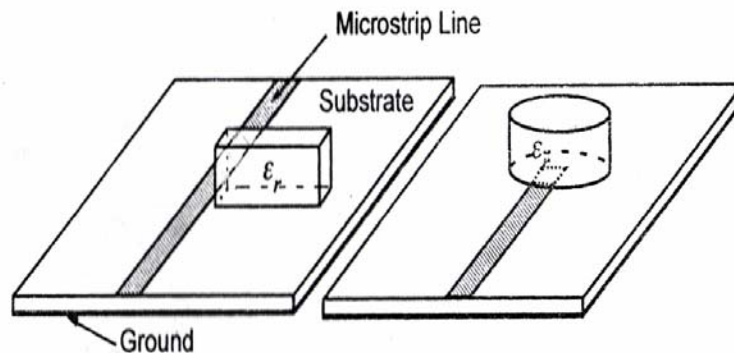


**Figure 2.5: Microstrip line coupling to DRA (Petosa, 2007)**

### 2.3.2 Coaxial Probe

Probe coupling is another common method to excite DRA. One advantages of coaxial probe excitation is the direct coupling to the  $50 \Omega$  system and useful at lower frequency application where aperture-coupling may not be practical. However, it need hole to be drilled whether to the substrate or to the DRA resulting air gap problem. The way to optimize its coupling is by adjusting the probe height and its location (Petosa, 2007). Figure 2.6 shows this type of coupling.

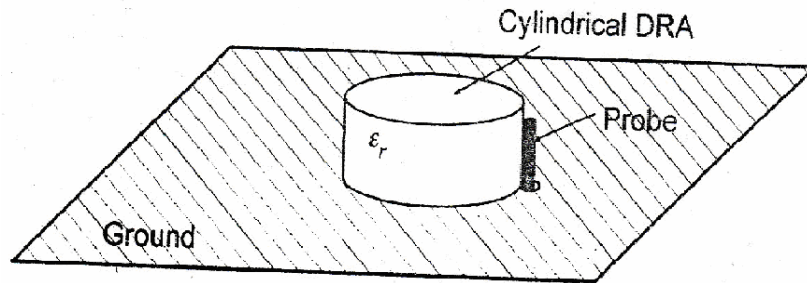


**Figure 2.6: Probe coupling to DRA (Petosa, 2007)**

### 2.3.3 Slot Aperture

DRA can also be excited through an aperture in the ground plane which can be feed by a transmission line (microstrip or coaxial) or a waveguide. This aperture can be designed in different shape with rectangular slot is probably the most widely used. Normally, the amount of coupling can be controlled by properly selecting the length and width of the slot and varying the position of DRA on the slot. It offers advantage from the other method due to the isolated radiating aperture from the feed preventing itself from any unwanted coupling (Petosa, 2007). Figure 2.7 shows slot aperture coupling to DRA.

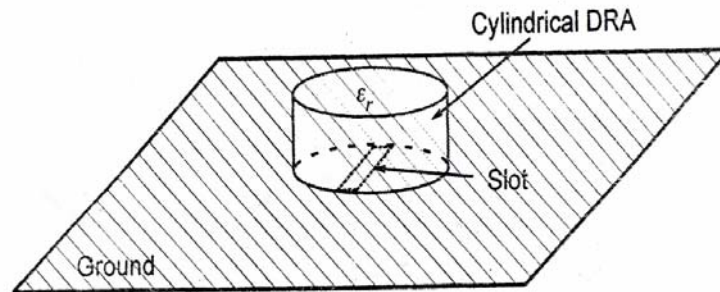


**Figure 2.7: Slot aperture coupling to DRA (Petosa, 2007)**

### 2.3.4 Coplanar waveguide

Coupling to DRAs can also be accomplished by the way of coplanar feeds. It offers additional control for impedance matching by introducing stubs or loops at the end of microstrip line. The way to control the level of coupling is by adjusting the position of DRA over the loop (Petosa, 2007).

### 2.3.5 Dielectric Image Guide

Dielectric image guide (DIG) is another method of coupling but seldom being used in application because it occupies extra space contributing to more complex design. The amount of coupling can be controlled by adjusting the spacing between DIG and dielectric resonator. DIG offer advantages as compared to microstrip line coupling in millimeter – wave frequencies due to the minimum conductor losses. Besides, DIG is the most suitable coupling when it comes to excite a linear array of DRAs (Petosa, 2007).

## 2.4 Analyses of the DRA

### 2.4.1 Resonant Frequency

Long et al., (1983) carried out simple analysis for the fields inside the cylinder DRA using magnetic wall model in order to analyze the field inside the DR and predict the resonant frequency. The analysis is done on the cylindrical DRA as shown in the Figure 2.1. In this analysis, the feed probe is temporarily ignored and the cylinder is completely isolated. The wave function which are transverse electric and transverse magnetic to z can be written as

$$\psi_{TE_{npm}} = j_n \left( \frac{X_{np}}{a} p \right) \begin{Bmatrix} \sin n\phi \\ \cos n\phi \end{Bmatrix} \sin \left[ \frac{(2m+1)\pi z}{2d} \right] \quad (2.1)$$

$$\psi_{TM_{npm}} = j_n \left( \frac{X'_{np}}{a} p \right) \begin{Bmatrix} \sin n\phi \\ \cos n\phi \end{Bmatrix} \cos \left[ \frac{(2m+1)\pi z}{2d} \right] \quad (2.2)$$

Where  $J_n$  is the Bessel function of the first kind, with  $J_n(X_{np})=0$ ,  $J'_n(X_{np})=0$ ,  $n=1, 2, 3\dots$   $p=1, 2, 3\dots$   $m=0, 1, 2, 3\dots$

Resonant frequency can be predicted from this separation equation in the Equation 2.3

$$k_r^2 + k_z^2 = \epsilon_r \left( \frac{2\pi f}{c} \right)^2 \quad (2.3)$$

where  $c$  is the velocity of light in free space and  $f$  is frequency.  $k_r$  and  $k_z$  are the wavenumbers inside the cylindrical DR in  $r$  and  $z$  directions respectively and their Equation are

$$k_r = \frac{X_{vp}}{a} \quad (2.4)$$

$$k_z = \frac{(2m+1)}{2d} \pi \quad (2.5)$$

By rearrangement from Equation 2.3, the resonant frequency of a mode  $f_{\text{vpm}}$  is given as

$$f_{\text{vpm}} = \frac{c}{2\pi\sqrt{\epsilon_r}} \sqrt{k_r^2 + k_z^r} \quad (2.6)$$

and when substitute both Equation 2.4 and 2.5 into Equation 2.6 , the resonant frequency is given as

$$f_{\text{vpm}} = \frac{c}{2\pi\sqrt{\epsilon_r}} \sqrt{X_{\text{vp}}^2 + \left[ \frac{\pi a}{2d} (2m+1) \right]^2} \quad (2.7)$$

where  $X_{\text{vp}}$  is the root satisfying the characteristic equation.

### 2.4.2 Resonant Modes

DRA can excite different modes with different radiation characteristic. These modes can be generated by the proper excitation mechanisms (Kishk, 2003). The modes of a cylindrical DRA are of TE, TM and hybrid type, while for spherical DR, the modes are TE and TM types (O'Keefe et al., 2002). For the hybrid mode, it is called HE if the  $E_z$  component is dominant or EH if the  $H_z$  component is dominant. The modes which are most commonly used in the radiating application are the  $\text{TM}_{01}$ ,  $\text{TE}_{01}$  and  $\text{HE}_{11}$  (Petosa, 2007). In such shielded environment,  $\text{TE}_{01}$  mode is often used while in radiating environment  $\text{HEM}_{11}$  mode is applied (Kajfez and Kishk, 2002). Different modes have different field distribution inside the DR and are assigned with three indexes such as  $\text{TE}_{018}$  and  $\text{TM}_{018}$  (Fiedziuszko, 2001).



The first index denotes the number of azimuthal variations and second index represent the number of radial variations. The third index,  $\delta$ , represent that the DR is shorter than one-half wavelength and is seldom to be used, thus, this index is often neglected. The electromagnetic field is circularly polarized if the first index is zero and normally is classified as  $TE_{0n}$  and  $TM_{0n}$  (Kajfez and Kishk, 2002). Figure 2.8 shows electromagnetic field for  $TE_{01}$ . The other resonant modes are all of the hybrid nature if the first index is bigger than zero which can be classified as  $HEM_{mn}$ . The hybrid mode with the lowest resonant frequency is  $HEM_{11}$  as shown in the Figure 2.9.

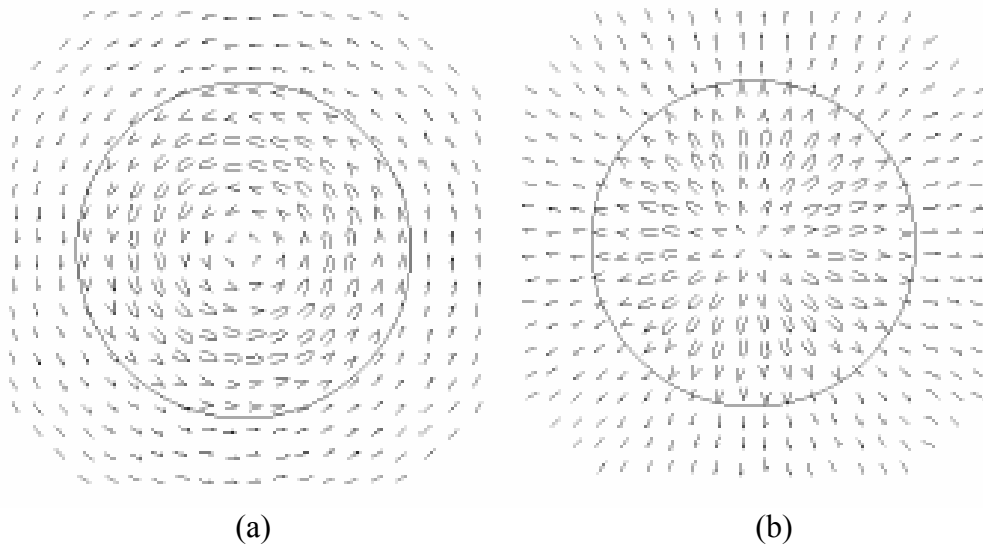


**Figure 2.8: Electric field distribution for  $TE_{01}$  (a) E-field (b) H-field (Kajfez and Kishk, 2002)**

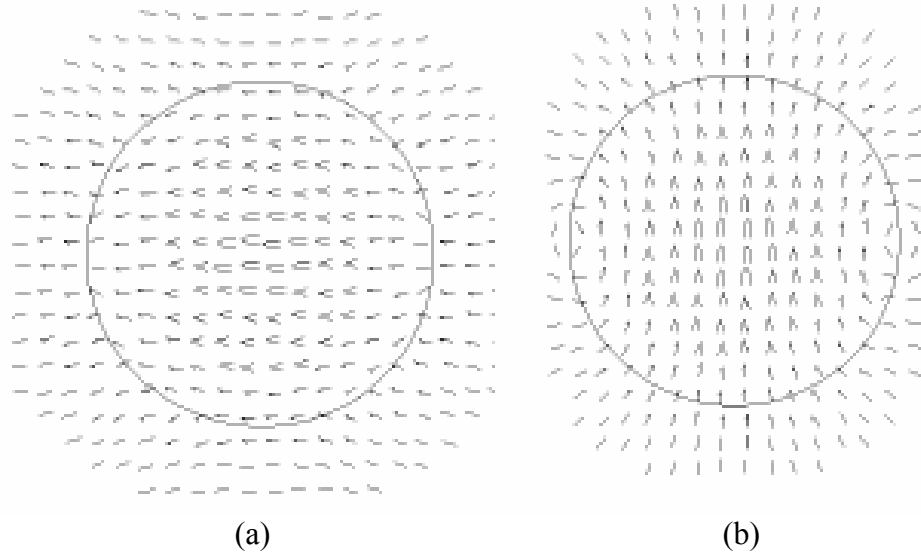


**Figure 2.9: Electric field distribution for HEM<sub>11</sub> (a) E-field (b) H-field (Kajfez and Kishk, 2002)**

Excited mode within DRA is closely related to the type of feeder being used. It is because the method of feeder and its location play important role to determine the type of modes. Consequently, input impedance and the radiation characteristic of the DRA can also be obtained. Therefore, it is essential to have the knowledge and good understanding of the internal field distribution of the isolated DRA to determine where the feed should be placed to generate the desired mode (Kajfez et al., 1984; Petosa, 2007). For the mode HEM<sub>11</sub>, side view of electric field distribution as shown in the Figure 2.10 (a) indicates that electric field is parallel to the interface of the isolated DR. Magnetic field distribution as in the Figure 2.10 (b) represent the top view of the HEM<sub>11</sub> mode.

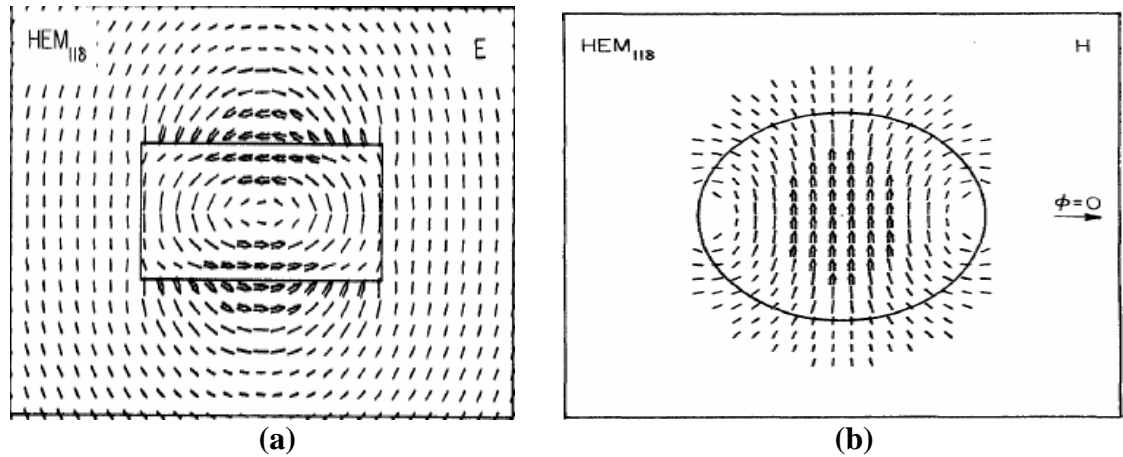


**Figure 2.10: HEM<sub>11</sub> mode (a) Electric field distribution (b) Magnetic field distribution (Kajfez et al., 1984)**

In order to excite this mode properly by using coaxial cable, the inner conductor should be inserted at the edge or slightly inside the DRA as shown in the Figure 2.11. If rectangular DRA is excited by coaxial cable, TE<sub>11</sub> mode can be generated (Kajfez et al., 1984; Petosa, 2007).

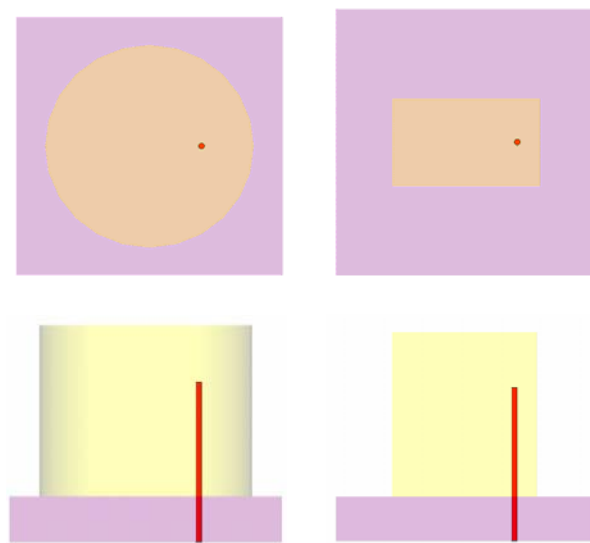


**Figure 2.11: Structure of probe feed cylindrical and rectangular DRA (O'Keefe et al., 2002)**